Modal Analysis of Waveguide Antennas With Arbitrary Cross Sections

Rainer Kühne and Jürgen Marquardt, *Member, IEEE*

***Abstract*—An approach is given to analyze the modal coupling of open-ended waveguides with arbitrary cross sections located in a conducting screen. The presented theory enables the determination of reflection characteristics of a single waveguide, as well as the analysis of mutual coupling between elements in waveguide antenna arrays. The field inside each waveguide is expressed as a sum of the transverse-electric and transverse-magnetic modes and expressions for the mutual admittances of modes excited at the aperture are obtained using a direct integration method. From these expressions, the mode reflection and conversion coefficients are determined. Computed and measured results are presented. Furthermore, this approach has been used to design a new type of horn antenna with high return loss and equal radiation patterns in the two principle planes.**

***Index Terms*—Horn antenna array, mutual coupling, open-ended waveguide.**

I. Introduction

WAVEGUIDES and horns with rectangular, circular, and elliptical cross sections are widely used as elements for waveguide antenna arrays. The open end and the mutual coupling do effect the element impedance and the radiation pattern by causing the complex amplitude of modes to differ from that of isolated elements. For an accurate prediction of the antenna or array performance, this modal coupling should be included in any design procedure. It can be analyzed very accurately using an integral equation and a Green's function approach.

In the past, only the cross sections mentioned above were taken into account to determine the mutual coupling of waveguide elements [1]–[3]. This paper deals with a more general approach for the eigenmodes of the waveguides, which allows to take into consideration nearly any kind of cross section, e.g., a square cross section with rounded corners. The main reason for applying these elements is obvious: if the antenna should consist of a square waveguide or horn, but should also be milled from one workpiece with an axially introduced milling tool, certain roundings will necessarily remain in the corners of the square cross section. These roundings influence the cutoff frequencies and field distributions of all modes, which means that they influence the scattering parameters as well as the beam shape, sidelobe level, and driving impedance.

II. Formulation

Consider the N cylindrical waveguides terminating in a common ground plane illustrated in Fig. 1. The aperture field of each waveguide can be approximated as a sum of $M(i)(i = 1,\ldots,N)$ modes. In terms of the incident wave amplitudes at the apertures, the amplitudes of the reflected waves are $\boldsymbol{b} = \boldsymbol{S}\,\boldsymbol{a}$, where $\boldsymbol{S} = 2(\boldsymbol{U} + \boldsymbol{Y}^{-1}) - \boldsymbol{U}$ is the modal scattering matrix of the complete array environment, $\boldsymbol{U}$ is the unity matrix, and $\boldsymbol{Y}$ is the admittance matrix; $\boldsymbol{a}$ and $\boldsymbol{b}$ are the column vectors of the incident and reflected mode amplitudes. The elements of $\boldsymbol{Y}$ represent the mutual admittance of modes m and n in apertures i and j, respectively. They can be calculated by the formula

$$y_{ij}(m,n) = \frac{jkY_0}{2\pi\sqrt{Y_m Y_n}} \int\int_{S_i} \boldsymbol{\Psi}_m \cdot \int\int_{S_j} \boldsymbol{\Psi}_n\, G(x-x_j, y-y_j)\, dS_j\, dS_i \quad (1)$$

where

Y_0 wave admittance in the half-space $= \sqrt{\epsilon_0/\mu_0}$;
Y_m wave admittance of waveguide mode m;
k wavenumber in the half-space $= \omega\sqrt{\epsilon_0\mu_0}$;
$\boldsymbol{\Psi}_m$ $\boldsymbol{h}_{tm} + k_{zm}/k \cdot h_{zm}\,\boldsymbol{e}_z$.

This formula is based on the field equivalence principle, the image theory, and a Galerkin method. ϵ_0 and μ_0 are the permittivity and permeability of the external region, ω is the angular frequency, $\boldsymbol{h}_{tm}$ and h_{zm} are the transverse and axial magnetic fields of mode m, k_{zm} is the wavenumber of mode m, and $G(x,y) = \exp(-jkR)/R$ is the scalar Green's function with $R = \sqrt{x^2+y^2}$.

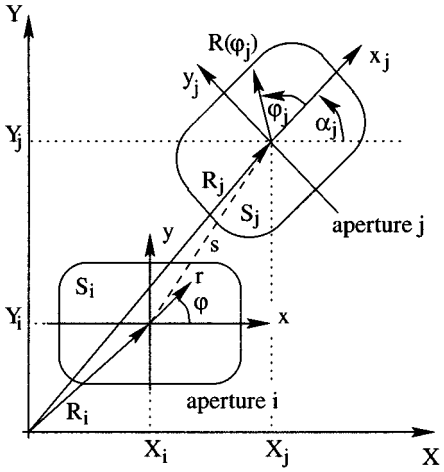

Fig. 1. Geometry of cylindrical waveguides opening into a common ground plane.

Manuscript received February 20, 2001.

The authors are with the Institute of High Frequency Technology, University of Hanover, 30167 Hanover, Germany (e-mail: kuehne@hft.uni-hannover.de).

Publisher Item Identifier S 0018-9480(01)09375-9.

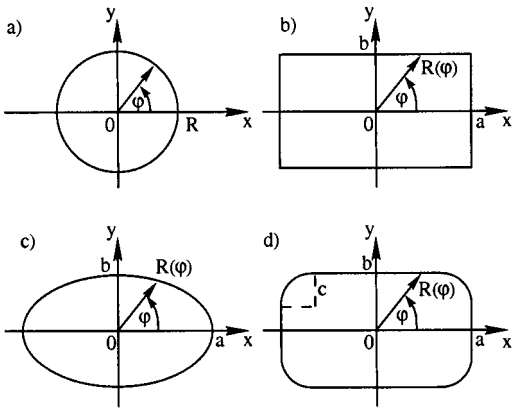

Fig. 2. Cross sections of cylindrical waveguides.

A. Waveguides With Arbitrary Cross Sections

The computation of (1) requires the knowledge of the field distribution of the eigenmodes of the waveguides. The calculation of the eigenmodes is based on the expansion of the fields into basic solutions of the wave equation in polar coordinates [4]. Therefore, the steady contour of each waveguide has to be formulated in polar coordinates. This and symmetry to the two principle planes are the only prerequisites for its cross section. Thus, it is possible to describe a wide variety of waveguides, e.g., a rectangular waveguide with rounded corners, illustrated in Fig. 2(d). The radius of the rounded corners may be very small (e.g., in order to have a closer look at the deviations from an ideal rectangular waveguide that have to be expected), but may also take the maximum size of half the height of the waveguide in question. For the special case of a square waveguide, the last item generates a circular cross section (see Fig. 2(d) with $a = b = c$).

The normalized scalar potentials for each waveguide (infinite conductivity is considered) have the following form for TE_m (or H_m) modes

$$F_{zm} = N_m \sum_{p=0}^{\infty} C_{pm} J_p(k_{cm} r) \cos(p\varphi - \psi_m) e^{-jk_{zm}z} \quad (2)$$

and for TM_m (or E_m) modes

$$A_{zm} = N_m \sum_{p=0}^{\infty} C_{pm} J_p(k_{cm} r) \cos(p\varphi - \psi_m) e^{-jk_{zm}z}. \quad (3)$$

Unlike the customary indication of the modes with two index numbers, only one index number can be given here since there is not a sole basic function per mode, but instead a infinite number has to be assumed. That is why the index number also gives no clear indication of the appropriate field distribution.

With $k_{cm}^2 = k^2 - k_{zm}^2$, (2) and (3) satisfy the boundary conditions and $\mathbf{\Psi}_m$ can be expressed in rectangular components, as described in [5] and [6]. N_m is the normalization constant of mode m, C_{pm} are the expansion coefficients, J_p is a Bessel function of order p, and k_{cm} is the cutoff wavenumber of mode m. The polarization angle ψ_m is defined relative to the initial line in the local polar-coordinate system (r, φ) that is parallel to the y-axis for TE modes and parallel to the x-axis for TM modes. For a numerical computation, it is evident that the considered sum of the basic solutions of the wave equation in (2) and (3) has to be limited. As a rule, an upper limit of $p_{\max} = 9$ and $p_{\max} = 15$ is sufficient to calculate the cutoff wavenumber of the dominant mode and higher order modes for most waveguide cross sections, respectively. In Table I, the cutoff wavenumber of several TE and TM modes for a square waveguide are listed with the radius of the rounded corners as a parameter. As one can see, the results for a square and a circular cross section are in good agreement with the exact solutions. Note that, for a circular cross section, only one basic solution of the wave equation has to be considered.

TABLE I
COMPARISION OF COMPUTED NORMALIZED CUTOFF WAVENUMBER $k_c b$ AND EXACT SOLUTION FOR $b/a = 1$ (FOR a, b, c SEE FIG. 1)

mode		TE_1	TE_6	TM_2	TM_6
square		1.570796	4.712390	3.512407	6.47656
	0	1.570801	4.712408	3.512415	6.47659
	0.25	1.591172	4.758722	3.515110	6.48109
c/b	0.5	1.647432	4.849694	3.542753	6.52327
	0.75	1.731758	5.032082	3.635977	6.66845
	1	1.841184	5.331443	3.831706	7.01559
circular		1.841184	5.331443	3.831706	7.01559

B. Modal Coupling

For modes coupling within the same aperture, it is apparent from (1) that there is a singularity in the Green's function that must be treated very carefully for accurate results. One way of doing this is to substract the singularity out of the source region indicated in (4)

$$\begin{aligned} I &= \int\int_{S_j} \mathbf{\Psi}_n \, G \, dS_j \\ &= \int\int_{S_j} \mathbf{\Psi}_n \, [G - G_0] \, dS_j + \int\int_{S_j} \mathbf{\Psi}_n \, G_0 \, dS_j \end{aligned} \quad (4)$$

where $G_0 = 1/\mathrm{sqrt}[(x - x_j)^2 + (y - y_j)^2]$ is the static field Green's function. For evaluating the second integral, it is efficient to choose polar coordinates (t, θ) with the origin at the field point (x, y) (see Fig. 3). After changing the variables to $x_j = x + t\cos\theta$ and $y_j = y + t\sin\theta$, the integral can be written as

$$I = \int_0^{2\pi} \int_0^{t(\theta)} \mathbf{\Psi}_n \, dt d\theta \quad (5)$$

where $t(\theta) = \mathrm{sqrt}[(R(\varphi_j)\cos\varphi_j - x)^2 + (R(\varphi_j)\sin\varphi_j - y)^2]$ is the corresponding upper limit of the radial integration. Since the contour of the aperture is known only by a pair of variables $(R(\varphi_j), \varphi_j)$, one has to express $t(\theta)$ in terms of $R(\varphi_j)$ and φ_j. This leads to an equation of the form

$$R(\varphi_j)\sin(\varphi_j - \theta) - r\sin(\pi - \varphi + \theta) = 0 \quad (6)$$

which has to be fulfilled by a variation of φ_j. During the integration, this problem occurs once for each integration angle θ.

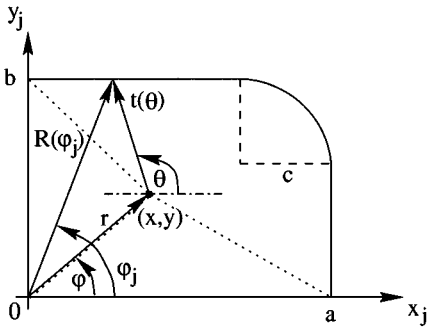

Fig. 3. Coordinate transformation for coincident apertures.

Though this procedure is valid for (x, y) inside the whole region of integration, it is necessary to subdivide this area to achieve an unambiguous relationship between $t(\theta)$ and φ_j. The easiest way to do this is to deal with one quadrant after the other and to subdivide each quadrant into the regions defined by the dotted lines in Fig. 3. Nevertheless, care must be taken of the interdependence of the variables and of the case where the field point (x, y) reaches the boundary.

When the two apertures are separate, numerical integration can be performed without difficulty. However, reduction of the fourfold integration in (1) to lower orders of integration has not been proven possible because of the interdependence of the integral limits and integration variables.

III. Results

The presented approach has been applied to calculate the mismatch of a single open-ended waveguide (OEW) due to the open end as well as the mutual coupling between different elements in waveguide antenna arrays. The computed results for the reflection coefficient of a single square waveguide with various roundings are shown in Fig. 4. The effect of the rounded corners can easily be seen. Measurements of the mismatch of an OEW have been performed with a circular (18.6-mm diameter) and a rectangular waveguide with rounded corners opening into a conducting screen (see Fig. 5).[1] The rectangular waveguide ($a = 12.5$ mm, $b = 5$ mm, $c = 5$ mm) was driven by a WR90. The scattering matrix of the discontinuity was calculated using a mode-matching technique and was combined with the scattering matrix due to the open end, which was calculated with the presented theory. A representation of the aperture field with $M = 4$ modes shows excellent agreement with the measured data in both cases. The reflection coefficient of the rectangular waveguide with rounded corners is slightly different compared to a WR90 shown in [6], mostly due to the different cutoff frequency, which is lower for the WR90.

Figs. 6 (using $M = 4$ relevant modes) and 7 (using $M = 8$ relevant modes) show the results for the coupling coefficient of the dominant mode for two waveguides located in the E- and H-plane with a spacing s and c as a parameter, respectively. As one can see, the radii of the rounded corners do have an influence on the coupling level. In the case where the two wave-

[1]Thickness of conducting screen: 6 mm for circular and 14 mm for rectangular waveguide with rounded corners. To reduce edge diffraction effects, microwave absorbing material was attached to the edges.

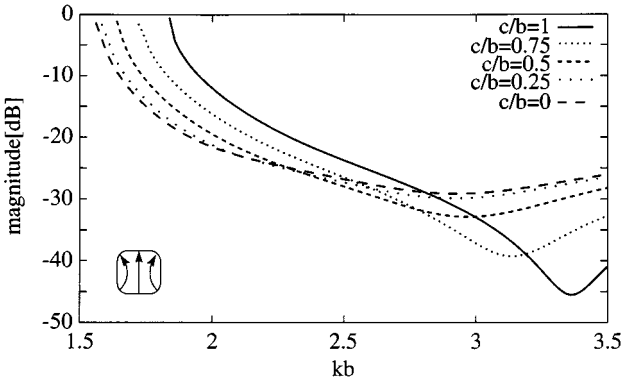

(a)

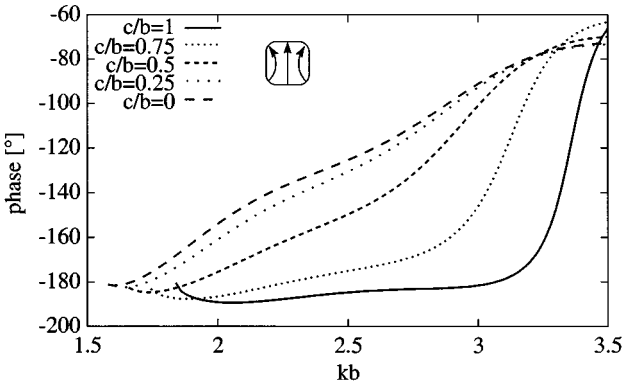

(b)

Fig. 4. Magnitude and phase of the reflection coefficient of the dominant mode against normalized frequency kb for $b/a = 1$.

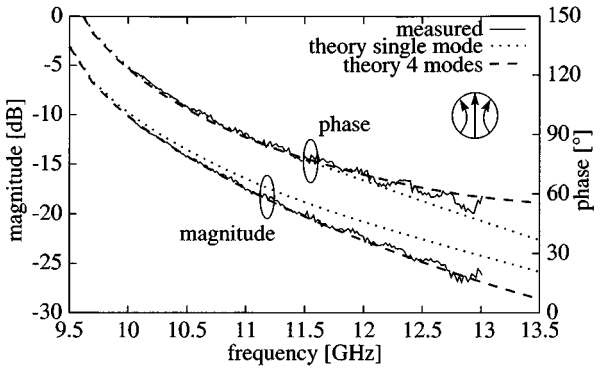

(a)

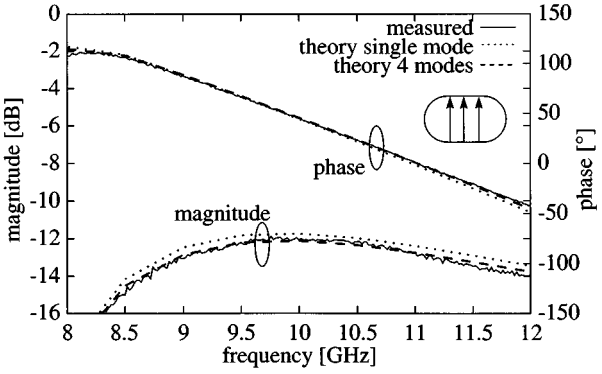

(b)

Fig. 5. Mismatch of a circular and rectangular waveguide against frequency.

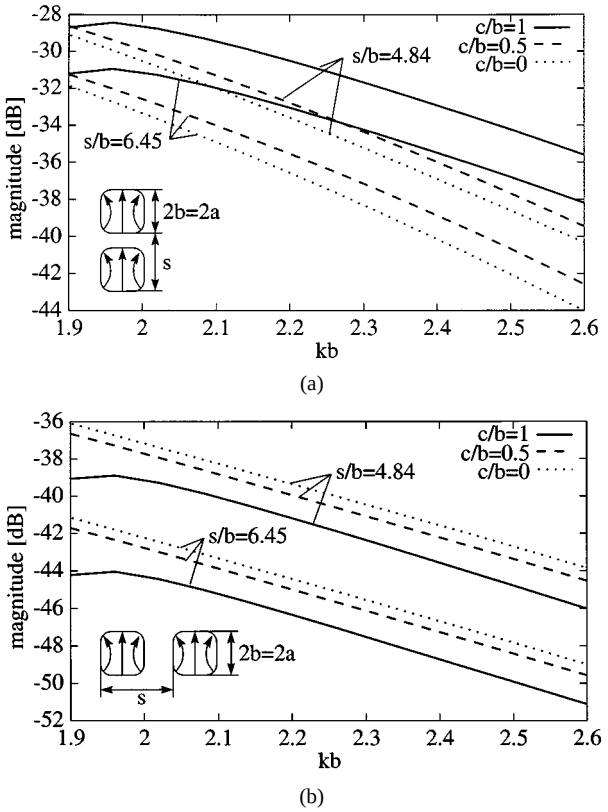

Fig. 6. E- and H-plane coupling of identical waveguides against normalized frequency.

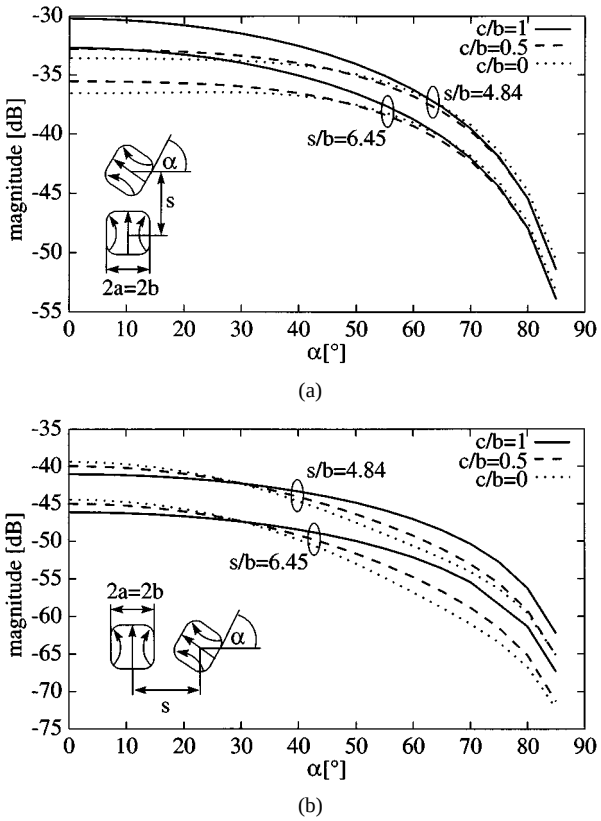

Fig. 7. E- and H-plane coupling of identical waveguides against rotation angle α at $kb = 2.2$.

guides are located in the E-plane, the mutual coupling of circular waveguides is higher than that of square waveguides. In the H-plane case, the result is reversed. It is clearly seen that the frequency dependence is not only shifted due to the cutoff frequencies.

Measurements for the coupling coefficient have been performed using the predescribed mechanical arrangement again. Two open-ended circular waveguides with $a = b = 9.3$ mm and $c/b = 1$ were located in the conducting screen with a spacing s. For this purpose, a full two-port calibration was carried out. The magnitude of the coupling coefficient of the dominant mode is shown in Fig. 8 and, again, the simulated data correspond very well with the measurements. The mutual coupling between two rectangular waveguides with rounded corners is shown in Fig. 9 for E-plane dispositions only. As the aperture field distribution is very similar to a waveguide with sharp corners, the mutual coupling is only slightly different compared to the case of two WR90's (i.e., shown in [6]).

Furthermore, Fig. 10 shows the geometry of a horn antenna, which consists of three square waveguide segments with rounded corners. An optimization process has been applied to achieve the following items. The antenna should be millable out of one piece and should be driven by a square waveguide. The return loss should be as high as possible and the radiation pattern in the two principle planes (@10.8 GHz) should be equal. The antenna itself was calculated using a mode-matching technique and, for the radiating aperture, the presented theory was applied and the two scattering matrices were then combined. Fig. 11 show the results of the optimization. The radiation patterns

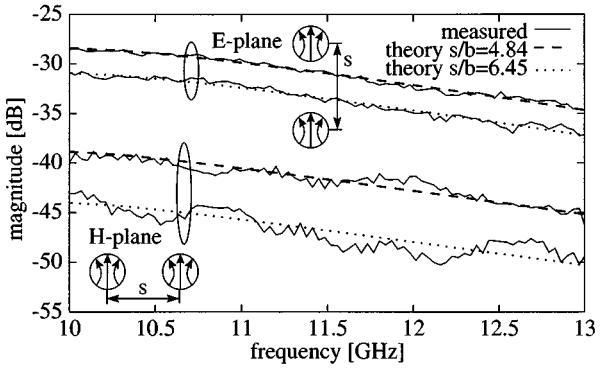

Fig. 8. Mutual coupling of circular waveguides ($a = b = c = 9.3$ mm).

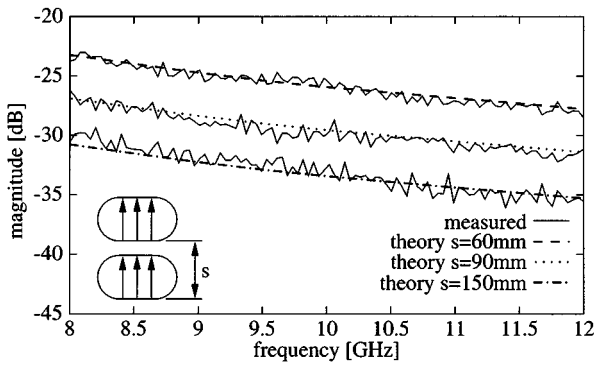

Fig. 9. Mutual coupling of rectangular waveguides with rounded corners each driven by a WR90.

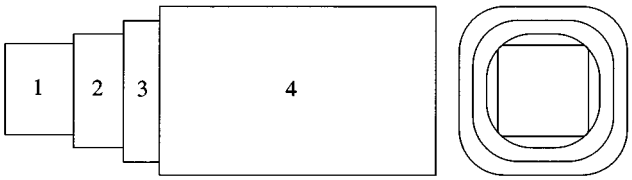

1: 20mm x 20mm c=0mm (driving waveguide)
2: 25.5mm x 25.5mm c=8mm l=11.36mm
3: 31.0mm x 31.0mm c=8mm l=7.43mm
4: 37.0mm x 37.0mm c=8mm l=61.30mm

Fig. 10. Geometry of the horn antenna.

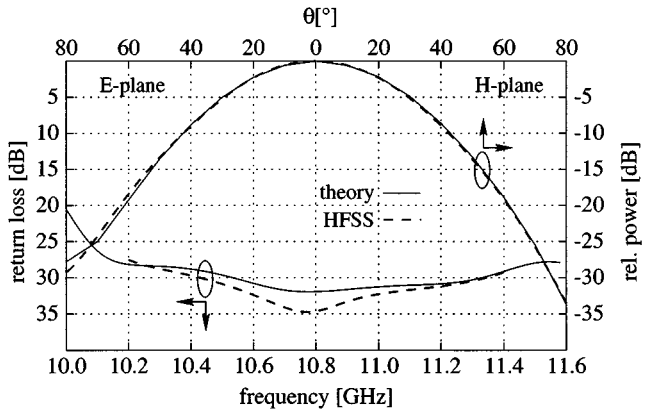

Fig. 11. Return loss against frequency and radiation pattern in the two principle planes (@10.8 GHz) of the horn antenna in Fig. 10 (directivity: 12.5 dBi, maximum cross-polar level: −24.5 dB).

are equal up to 70° and the return loss is higher than 30 dB. A verification with HFSS shows nearly the same results.

IV. Conclusion

An analysis of mode coupling in a finite array of waveguides with arbitrary cross sections opening into a ground plane has been presented. The approach is also valid for the calculation of a single OEW. In the case that a horn antenna has to be analyzed, the feeding structure can be calculated using a mode-matching technique. For the radiating aperture, the presented theory can be applied. The two scattering matrixes are then combined to one overall matrix, which indicates the reflection and, in the special case of an array analysis, the coupling effects. The presented approach has been applied to calculate the mismatch of a single OEW due to the open end, as well as the mutual coupling between two identical OEWs. Nevertheless, the presented formulation may also be applied to dissimilar apertures and waveguides with different cross sections within the same array. The theory was verified through several measurements with circular and rectangular waveguides. Furthermore, the optimized design of a new type of horn antenna with high return loss and equal radiation pattern in the two principle planes has been presented. The primary aim of this analysis is to provide a higher flexibility in the design process.

References

[1] T. S. Bird, "Improved solution for mode coupling in different-sized circular apertures and its application," *Proc. Inst. Elect. Eng.*, vol. 143, pp. 457–465, June 1996.

[2] T. S. Bird and D. G. Batemann, "Mutual coupling between rotated horns in a ground plane," *IEEE Trans. Antennas Propagat.*, vol. 42, pp. 1000–1006, July 1994.

[3] T. S. Bird, "Behavior of multiple elliptical waveguides opening into a ground plane," *Proc. Inst. Elect. Eng.*, pt. H, vol. 137, pp. 121–126, Feb. 1990.

[4] J. Marquardt and M. Schneider, "Waveguide circuits with nearly arbitrary cross sections," in *Int. Microwave Millimeter Wave Tech. Conf.*, Beijing, China, 1998, pp. 557–560.

[5] R. Kühne and J. Marquardt, "Mutual coupling of open-ended waveguides with arbitrary cross sections located in an infinite ground plane," presented at the European Microwave Conf., Paris, France, 2000.

[6] ——, "Coupling effects in finite arrays of open-ended waveguides with arbitrary cross sections," presented at the Asia–Pacific Microwave Conf., Sydney, Australia, 2000.

Rainer Kühne was born in Hanover, Germany, in 1970. He received the Dipl.-Ing. (M.S.) degree in electrical engineering from the University of Hanover, Hanover, Germany, in 1996, and is currently working toward the Ph.D. degree at the University of Hanover.

Since 1996, he has been a Research Assistant at the Institute of High Frequency Technology, University of Hanover. His research interests involve waveguide and horn antennas, as well as coupling effects in antenna arrays.

Mr. Kühne was the joint recipient of the Best Student Paper Prize presented at the 2000 Asia–Pacific Microwave Conference.

Jürgen Marquardt (M'94) was born in Göttingen, Germany, in 1936. He received the Dipl.-Ing (M.S.) and Dr.-Ing. (Ph.D.) degree in electrical engineering from the University of Braunschweig, Braunschweig, Germany in 1966 and 1971, respectively.

From 1971 to 1979, he was with the Research and Development Laboratories, ANT, Backnang, Germany, where, in 1974, he became Head of Department of Microwave Components. Since 1980, he has been a Professor of microwave engineering at the Institute of High Frequency Technology, University of Hanover, Hanover, Germany.